The first and third uORFs in RSV leader RNA are efficiently translated: implications for translational regulation and viral RNA packaging

Donze, Olivier; Damay, Pascal; Spahr, Pierre-François

How to cite

DONZE, Olivier, DAMAY, Pascal, SPAHR, Pierre-François. The first and third uORFs in RSV leader RNA are efficiently translated: implications for translational regulation and viral RNA packaging. In: Nucleic Acids Research, 1995, vol. 23, n° 5, p. 861–868. doi: 10.1093/nar/23.5.861

This publication URL: https://archive-ouverte.unige.ch/unige:130900

Publication DOI: 10.1093/nar/23.5.861

Nucleic Acids Research, 1995, Vol. 23, No. 5 861–868

The first and third uORFs in RSV leader RNA are efficiently translated: implications for translational regulation and viral RNA packaging

Olivier Donzé*, Pascal Damay and Pierre-Francois Spahr

Department of Molecular Biology, University of Geneva, 30 Quai E. Ansermet, 1211 Geneva 4, Switzerland

Received September 1, 1994; Revised and Accepted January 24, 1995

ABSTRACT

Rous sarcoma virus (RSV) RNA leader contains three short upstream open reading frames. We have shown recently that both uORFs 1 and 3 influence *in vivo* translation of the downstream *gag* gene and are involved in the virus RNA packaging process. In this report, we have studied the translational events occuring at the upstream AUGs *in vivo*. We show that (i) the first and third AUGs are efficient translational initiation sites; (ii) ribosomes reinitiate efficiently at AUG3; and (iii) deletions in the intercistronic distance between uORF1 and 3 (which is well conserved among avian strains) prevent ribosome initiation at AUG3, thus increasing translation efficiency at the downstream AUG*gag*. The roles of the uORFs in translation and packaging are discussed.

INTRODUCTION

In eukaryotic cells, translation is usually initiated in a manner consistent with the ribosome scanning model (1). According to this model, the 40S ribosomal subunit and translation initiation factors bind to the 5′ end of mRNA and scan the RNA leader until they reach an AUG codon in the appropriate context. Subsequently, the 60S ribosome joins and initiates polypeptide chain elongation (2). The scanning model accounts for the effects of structural features within the 5′ untranslated region, such as secondary structure and open reading frames, which can strongly influence the efficiency of translation initiation. The presence of one or more upstream open reading frames (uORFs) has been shown to influence the translation of downstream ORFs. Initiation occurs preferentially at the upstream site, which in turn reduces initiation downstream due to the apparent inefficiency of reinitiation at internal AUG codons. Therefore, in most cases, uORFs inhibit downstream translation in proportion to the efficiency of their own translation (1). In a few cases, the coding capacity of the uORF was found to influence the downstream translation (3–6).

In Rous sarcoma virus, the 5′ leader contains three short open reading frames of 7, 16 and 9 codons in length. The three uORFs are conserved in length, and in the nucleotide sequence surrounding the initiation codons among the avian/leukosis viruses (7). These three elements are situated at different strategic places within the leader. The first and second uORFs are found within the proximal 5′ secondary structure-rich region while the third uORF is located close to the packaging signal (termed ψ), which is required for efficient recognition of the viral RNA by *trans*-acting factors (8–10). Previous studies have shown that AUG1 is the main ribosome binding site in the RSV leader (11–13) and that the encoded heptapeptide product is synthesized *in vitro* (14). Furthermore, mutations that alter the RSV leader AUGs increased downstream translation *in vitro* only slightly (15), yet have profound effects on viral replication (16–18). In a recent study, we characterized the role of the three uORFs present in the leader of Rous sarcoma virus (Prague C strain). We reported that uORF1 and 3 are key elements involved in the viral life cycle and act by regulating the efficiency of translation at the downstream AUG*gag* as well as the efficiency of viral RNA packaging (18). Mutation of either AUG1 or 3 has a profound effect on RNA encapsidation, inhibiting this process by 20–50-fold. We proposed a model whereby ribosomes first translate uORF1 and then subsequently reinitiate and pause at the AUG3. We postulated that initiation at the third AUG is the central step in the regulation of RNA packaging. Reinitiation at AUG3 would impede temporarily the flow of ribosomes on the RSV leader, clearing the ψ packaging sequence present in the leader just downstream of uORF3 (18).

In the present study, we examined this prediction of our proposed model *in vivo*. To this end, we looked at the translation initiation rates at each AUG present within the RSV leader RNA. The reporter gene firefly luciferase was fused to all constructs to allow quantitation of translational initiation rates at the different AUGs. The reinitiation hypothesis between uORF1 and 3 was also tested by altering the intercistronic distance. Our data reveal that uORF1 and 3 are efficient initiation sites for translation and strongly suggest that AUG3 is recognized by reinitiating ribosomes. We also showed the effects of these RSV RNA leader alterations on the efficiency of viral RNA packaging.

MATERIALS AND METHODS

Cell culture

Chicken embryo fibroblasts prepared from Spafas eggs (Gs^- and Chf^-: Norwich, CT, USA) were grown in Dulbecco-modified

*To whom correspondence should be addressed at present address: Department of Biochemistry, McGill University, 3655 Drummond Street, Montréal, Quebec H3G 1Y6, Canada

Eagle medium containing 5% fetal calf serum (Gibco Laboratories, Grand Island, NY) at 41°C in an atmosphere supplemented with 5% CO_2.

Bacterial strains

Escherichia coli DH5α and CJ236 were grown according to the instructions of the mutagenesis kit (Biorad). *E.coli* DH5α was rendered competent as previously described (19). Plasmid DNAs were purified from either small or large bacterial cultures by the alkaline lysis method and for transfection were further purified by precipitation with polyethylene glycol (PEG) (19).

Cloned DNAs

Plasmid pAPrc has already been described (20); it contains a non-permutated copy of the provirus RSV Prague C strain. Plasmid pAsPrc is a *SalI–EcoRV* subclone of pAPrc in pBR322 containing the entire leader and *gag* sequences. All the mutations were constructed in Bs*lead*, a 1167 bp *SphI* fragment of pAsPrc cloned in the phagemid vector Bluescribe (–) (Stratagene, San Diego, USA).

To construct the plasmid carrying the luciferase gene (Bs*luc*), the *BsmI–BamHI* fragment (with the ends filled by the Klenow fragment of DNA polymerase I) from pRSV*luc* (21) containing the luciferase gene was cloned by blunt end ligation into Bs*leadMin* to replace the *Hin*dIII fragment encoding the *gag* gene (the *Hin*dIII ends were similarly filled by Klenow prior to ligation). Bs*leadMin* carries the 1167 bp *SphI* fragment of pAsPrc in which the AUG initiator of the *gag* gene at position 380 has been mutated to TTC in order to create a *Hin*dIII site at the beginning of the *gag* gene (22). Bs*luc* contains the RSV leader fused to the luciferase gene, including 20 nucleotides (nt) of the luciferase leader. A 440 nt *Pst*I fragment from each Bs*lead* mutant was cloned into the corresponding site of Bs*luc* to replace the sequence derived from Bs*leadMin*.

Construction of mutants in RSV leader

The following oligonucleotides were synthesised on an Applied Biosystems 381 A DNA synthetizer and purified as previously described (23):

M3[189]: 3′-GCAGAGCGAATAAGCTCCTACCCTGCAGTTGGGAT-CATCTCCCCC-5′
SEL3: 3′-CTCCCCCGACGCCGAAATCCTCCCGTCTTC-5′
Del44: 3′-ATCAATCCCTTATCACCAAAGCCCCTCGCC-5′par
ORF1-luc: 3′-AACTACCGGCCTGGCAGCTAAGGGCTTCTGCG-GTTTTTGTAT-5′
ORF2-luc: 3′-CTGGGGCTGCACTATCAATCCCTTCTGCGGTTTT-TGTATTTC-5′
ORF3-luc: 3′-TGGGATCATCTCCCCCGACGCCGACTTCTGCGG-TTTTTGTATTTC-5′
AUG3luc: 3′-GCGAATAAGCCCCTCGCCTGCTACCTTCTGCGG-TTTTTGTATTTCTTTCCG-5′

All the mutants cited above were constructed as described previously (24).

The mutant Ins was made by digesting the Bs*lead* clone (20) with *Bst*EII (position 102). A *BglII–SalI* insert (from plasmid pSp73: Promega) was treated with mung bean nuclease and ligated to Bs*lead* to give pAsIns: two inserts in inverted orientation are present, adding 94 nt to the RSV leader. We performed the same scheme to construct InsDel from BsDel44. The same pSp73 insert was used and again a double insert was present in the construct, but in the same orientation. InsDel carries, thus, a 94 nt insert at position 102 in addition of the 44 nt deletion: the intercistronic distance in this construct is 184 nt instead of 134 nt. In Del58, we removed the 58 nt *Rsr*II–*Bst*EII fragment (positions 47 and 102, respectively). Del13 was constructed by digesting the Bs*lead* clone with *Bst*EII followed by treatment with mung Bean nuclease. We obtained a 13 nt deletion from nucleotides 96 to 108. The introduction of the mutations was confirmed by the dideoxy-chain termination method of DNA sequencing using T7 polymerase (Pharmacia) primed by a synthetic oligonucleotide complementary to the 3′ end of the RSV leader. The mutated fragments were cloned back into pAsPrc using the *Sph*I sites and then the *SalI–EcoRV* fragment was introduced into pAPrc (20).

Transfection

Cells either freshly prepared from embryos or frozen in the presence of glycerol were used for transfection after two to seven passages. Cells were transfected using the DEAE–Dextran procedure as described previously (18).

Protein analysis

Viral particles produced by the transfected cells were purified by ultracentrifugation through a 20% sucrose cushion and their protein content analyzed by immunoblotting with polyclonal antibodies against RSV CA (p27), as described previously (20).

Luciferase assay

Each 10 cm plate of transfected CEF was washed three times in phosphate-buffered saline without Ca^{2+} and the cells were harvested in 500 µl of lysis buffer (Promega). Cell debris was pelleted by centrifugation in a microcentrifuge for 5 min at 4°C. A 20 µl aliquot of extract was added to 100 µl of assay buffer (Promega) in a small test tube. Luciferase activity was measured in millivolts in a luminometer (Bioorbit) using the luciferase assay system (Promega).

Total luciferase RNA was isolated from transfected CEF using the guanidinium/CsCl method (19). RNA was then digested with DNase I and subjected to a RNase ONE protection (Promega) because RNA levels were too low for decisive Northern experiments. Prior to conducting the experiments shown in Figures 2 and 5, we evaluated this 'RNase One' by using different amounts of pure luciferase RNA (from Promega). The data from this experiment convinced us that this enzyme gave a linear and quantitative signal, although residual undigested probe was still present. To obtain protected fragment of the same size for luciferase constructs, a 413 RNA antisense probe was synthesized from the pGEM-luc (Promega) digested with *Eco*RV; this probe contains homologies to the last 356 nt of the luciferase ORF.

Purification of viral RNA

The viral RNA of virions produced after transfection was purified and analyzed by RNase protection assay. The RNA was extracted from virions as described previously(18). Total cellular RNA was purified from subconfluent cultures by lysis in guanidinium thiocyanate, followed by centrifugation through cesium chloride as described (19).

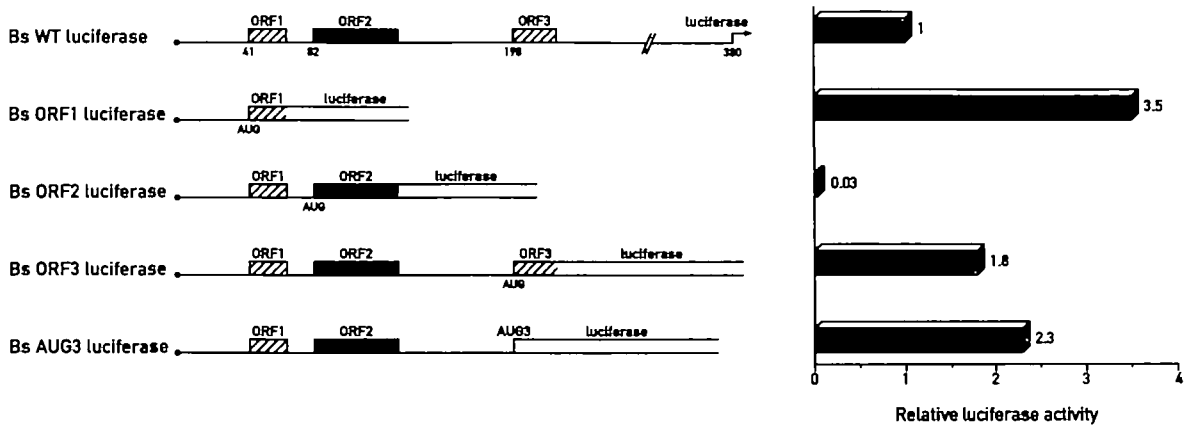

Figure 1. Efficiency of translation initiation at the different AUGs present in RSV leader. The schematic depicts the 5′ end encoded by the different luciferase fusion construct (drawn to scale). The uORFs are represented by boxes. The hatched boxes symbolize the uORFs involved in translation and packaging regulation (9). The numbers indicate the first AUG triplet for each uORF-luciferase fusion and the AUG initiator of the luciferase gene. Levels of luciferase activity are shown at the right and are given relative to the control plasmid with the whole RSV leader (BsWT-luciferase); values have been normalized to the RNA levels (Fig. 2). The light units produced by any given luciferase expression vector varied by <10% in parallel transfections using two independent clones for each construct. The emitted light was quantitated in a Bioorbit luminometer.

Quantitation of RNA present in the virions or in the cell were performed using an RNase-protection assay. Plasmid pL(–), which contains the *Eco*R1–*Xho*I fragment from pAPrC (20), was digested with *Sac*I and *in vitro* transcribed using T7 polymerase and a commercial kit (Promega) according to the kit instructions. The antisense RNA probe contains homologies to 355 nt of the leader and the *gag* gene. Plasmid pL(–) was also digested with *Bst*EII and *in vitro* transcribed using T7 polymerase. The antisense transcript produced was used to detect the presence of the mutations in viral RNA extracted from the different mutant virions (data not shown). RNase protection was performed with RNase One (Promega) as described by the manufacturer. The nuclease resistant hybrid was analysed on a denaturing polyacrylamide gel and the product detected by autoradiography.

RESULTS

Upstream AUG codons 1 and 3 in RSV leader RNA are efficient initiation sites

We showed previously that alterations of AUG1 or AUG3 present in the RSV leader RNA influences translation of the *gag* gene, situated downstream of the uORFs. uORF1 is a translational enhancer of viral proteins, while uORF3 inhibits downstream translation at the AUG*gag* (18). These results strongly suggested that ribosomes initiate and translate both uORF1 and uORF3 *in vivo*. To study further the translational events occuring at the RSV leader uORFs, we fused the end of each uORF to the coding sequence of the firefly luciferase gene (21). Fusion constructs have been successfully used for a better understanding of the uORFs present in the leader of the GCN4 gene in the yeast *Saccharomyces cerevisiae* (25). Since the luciferase coding region was fused at the end of the uORFs in order to minimize artifacts due to the fused gene, we reasoned that expression of the uORF–luciferase fusions should reflect the translational rates of unmodified uORFs (see Discussion). For each construct, we used two independent clones. The expression from each fusion construct was tested by transient transfection into chicken embryo fibroblasts (CEFs). To ensure that differences in luciferase activities observed were due to differential translational efficiencies rather than transcriptional variations, we monitored levels of luciferase RNA within the transfected cells by RNase protection analysis. A representative protection experiment is shown in Figure 2, using a probe which protected 356 nt of the luciferase mRNA. In several experiments, we observed similar levels of RNA synthesized from each construct, indicating that the variations in luciferase activity truly reflected altered translational efficiencies of the recombinant RNAs.

The luciferase activities in extracts from cells transfected with each construct were normalized to the activity in cells transfected with BsWT-luciferase construct, which contained the whole RSV leader fused to the luciferase sequence (Fig. 1 and ref. 18). Translational efficiency at the first AUG was measured in the BsORF1-luciferase plasmid which produced as much as 4-fold more activity than at the AUG*gag* (compare Bswtluc with BsORF1luc in Fig. 1). The luciferase activity present in the lysate of cells transfected with BsORF2-luciferase was no more than 3% of the activity observed at the AUG*gag* and even less if we compare to the efficiency at AUG1. This indicates that AUG2 is poorly recognized by ribosomes during the scanning process, in agreement with previous observations (18,29). To investigate initiation occuring at AUG3, we used two different fusion plasmids (Fig. 1): in the BsORF3-luciferase construct, the luciferase was fused to the end of the third reading frame, whereas in the BsAUG3-luciferase plasmid, the reporter sequence was directly fused to AUG3. Both constructs showed that AUG3 is an efficient initiation codon (2-fold increase compared to AUG*gag* in Bswtluc; Fig. 1). Although a precise comparison of the levels of expression of the fusion proteins could not be made without knowledge of differences in the stability and specific activity of each, the results support the idea that both uORF1 and uORF3 are sites for efficient translation initiation.

To rule out the possibility that luciferase activities observed were due to recognition of a cryptic initiation codon present within the luciferase coding region (21) rather than those within the RSV leader region, we mutated the initiation AUG into a non-initiation codon for each uORF fusion construct. The control

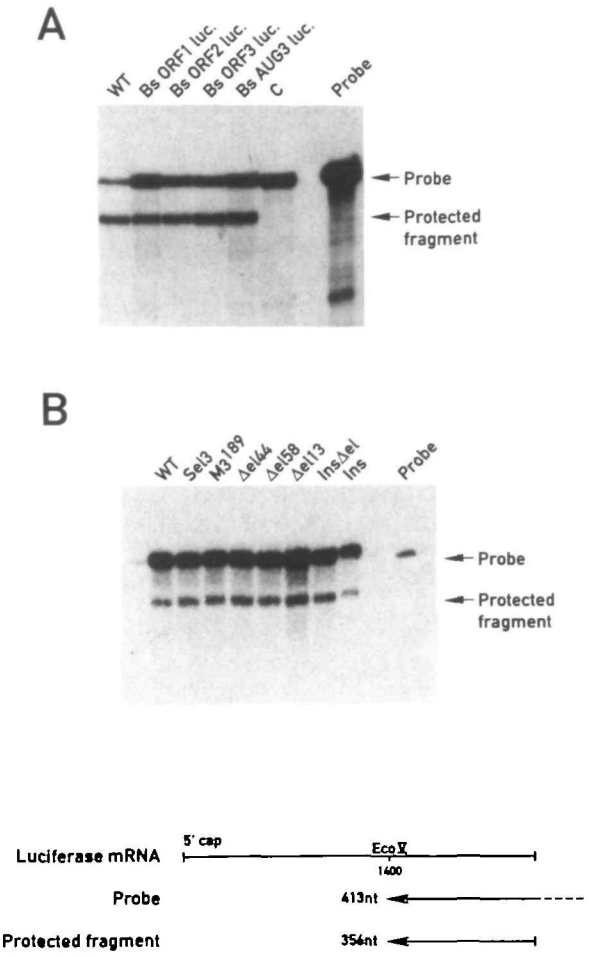

Figure 2. RNase protection analysis of luciferase containing mRNAs produced by the different Bsluciferase constructs. On the top is the analysis of protected fragments by electrophoresis in a polyacrylamide sequencing gel. Bands were visualized by autoradiography. Names of the different constructs designed in Figures 1 and 3 are shown above the corresponding lane. Undigested probes and protected fragments are indicated on the right. At the bottom is shown a schematic illustration of the probe used in this experiment. The *Eco*RV represents the 3′ end of the RNA probe.

constructs were transfected into CEFs and luciferase activity was monitored in the lysate of transfected cells. None of the cells transfected with control plasmids produced any detectable luminescence and as such were comparable to the luciferase activity from lysates of the mock-transfected cells (data not shown). This demonstrated that the luciferase data reported above reflect the use of the RSV leader AUGs.

Elongation of uORF3 diminished translation at the AUG*gag*

To investigate whether the initiation potential of AUG3 in the full-length virus leader parallels that of the luciferase-fusion construct, we lengthened uORF3 in the RSV leader by addition of a single base (a thymidine) at the end of uORF3 (Sel3: Fig. 3). This addition shifts the frame of the third uORF, leading to termination 11 codons downstream of the AUG*gag*. Since uORF3 in Sel3 overlaps the *gag* sequence, translation initiation at AUG3 codon is expected to interfere with initiation at the *gag* AUG codon (26–28). This was ascertained by studying the luciferase gene fused to the RSV leader. The Sel3 mutation did not affect the mRNA level as observed by RNase protection analysis (Fig. 2). As expected, the lengthened version of uORF3 affected the translational efficiency at AUG*gag*, causing a 3-fold decrease in luciferase activity compared to wild-type value (35% translation efficiency compared to WT) (Fig. 3). Together with results of uORF-luciferase fusion studies, these data point out the strong initiation potential of the third AUG, contradicting a previous study which showed indirectly that AUG3 is initiated to a small extent (29).

Insertion of a sequence with the potential to form stable secondary structures greatly inhibits protein expression initiated at AUG*gag*

The presence of a sequence with the potential to form stable secondary structures in the 5′ mRNA leader generally inhibits translation in eukaryotes, presumably because it interferes with the scanning process (30–32). In the case of poliovirus mRNA, evidence was presented that these negative elements are without effect as the mRNA is initiated by the process of internal initiation (33). To determine whether ribosomes can overcome such an inhibitory element in the RSV leader, we introduced a sequence capable of forming a stable secondary structure between uORF1 and uORF3 (mutant 'Ins' Fig. 3). This sequence was extremely stable (>150 Kcal/mol) and was formed by a 94 nt insert with dyad symmetry. When transcribed into mRNA, it is predicted to form a stable hairpin structure. We introduced this sequence at position 102 within the RSV leader which is 38 nt downstream from the uORF1 termination codon and 96 nt upstream from the uORF3 initiation site. Sequences with similar predicted secondary structure have been shown to reduce greatly cap-dependent translation in eukaryotic cells (30,32). As shown in Figure 3 (compare WT with Ins), the presence of this stable structure within the leader strongly inhibits translation initiation at the AUG*gag* (>1% of WT). The observed defect was manifested at the level of translation, since analysis of mRNA showed similar levels of transcript (Fig. 2). To test whether this insertion was inhibitory due to the stem structure or simply because of its particular sequence, we inserted the same sequence without dyad symetry in the same location (see Materials and Methods and Fig. 3: InsDel). The presence of this unstructured sequence does not affect translational efficiency at the AUG*gag*. This indicates that secondary structure in the Ins construct was responsible for the observed effect, rather than the sequence itself (compare Ins and InsDel: Figs 3 and 4). These data, taken together with the observations reported above, strongly suggest that translation of uORFs and of the *gag* gene occurs *in vivo* by a ribosome scanning along the RSV leader. These data also fit with previous results showing that *in vitro* a stable secondary structure present within the RSV leader decrease translation to 10% compared to the WT level (15).

Effect of intercistronic length between uORF1 and 3 on downstream translation

Efficient reinitiation is dependent on intercistronic length. It has been observed that inhibition of preproinsulin synthesis by an uORF increased as the intercistronic distance was decreased from 79 to 2 nt (34). In our system, the uORF1 and 3 are separated by 134 nt and this interval is well conserved between the different

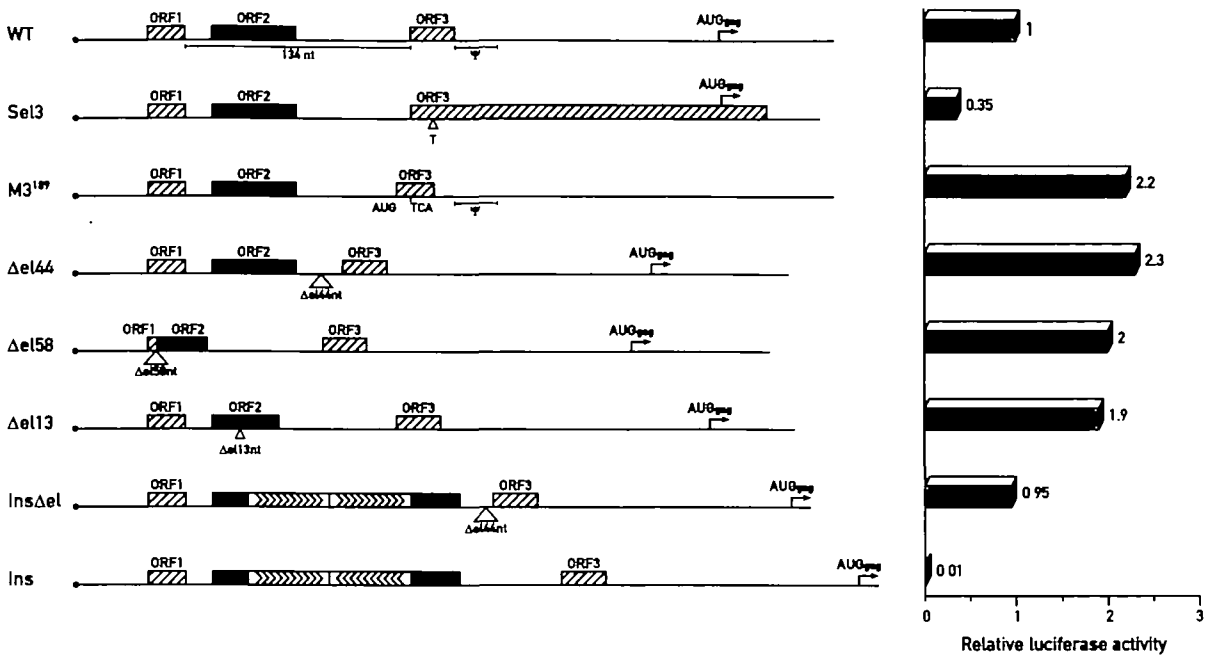

Figure 3. Translational efficiency of the mutants in the RSV leader. The scheme shows the different mutants with alterations in the intercistronic distance between uORF1 and uORF3 as well as in uORF1 and uORF3. The functional uORFs are represented in hatched boxes. Levels of luciferase activity are given relative to the control plasmid with the whole RSV leader (BsWT-luciferase). The light units produced by any given luciferase expression vector varied by <10% in parallel transfections (see Materials and Methods).

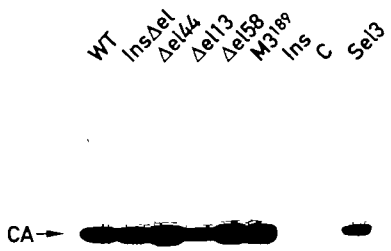

Figure 4. Analysis of the virion *gag*-encoded proteins. Virions produced by the transfected cells were purified as described in Materials and Methods. Viral proteins were resolved by SDS–PAGE and immunoblotted with polyclonal antibodies against RSV CA (p27) and detected with ^{125}I-labelled protein A. The mutants designated in Figure 3 are indicated above each lane. Lane C indicates the control cells, mock transfected with no DNA.

avian strains (7,35). If reinitiation occurs in the RSV leader, then decreasing the distance between uORF1 and uORF3 should allow ribosomes to bypass the uORF3, thus increasing translation efficiency downstream at the AUG*gag*, as observed in the absence of AUG3 (18). To test this possibility, several mutants with decreasing distance between both uORFs were made and two independent clones were used for each mutant (Fig. 3). The first construct (Del44) has a 44 nt deletion between the minicistrons (positions 137–181). Another carries a 13 nt deletion within the uORF2 (Del13); we chose to delete this region because the surrounding sequences are dispensable for regulation of both translation and packaging (36,37). Restriction sites present within the first (*Rsr*II) and second uORFs (*Bst*EII) were used to delete 58 nt and to create a new uORF beginning at AUG1 and terminating at the uORF2 stop codon. This mutant (Del58) possesses an uORF1 of 12 codons terminating at position 130, thus situated at 68 nt upstream of the third initiation codon. For mutant M3^{189}, AUG 3 was mutated to UCA (as in pAM3: 18) and a new AUG (in a good context for translation: AGGATGG) was created at position 189 to replace an AGC codon. In the latter case, translation of the new uORF3 would occur in a −1 frame producing a pentapeptide product. Moreover, the intercistronic interval was decreased by 11 nt in this mutant. The mutants Del44 and Del13 did carry intact uORF1 and 3, while the two other mutants, Del58 and M3^{189} have a modification in uORF1 or uORF3, respectively.

To evaluate the effect of these deletions on translation initiation at the AUGgag codon *in vivo*, we measured the emission of light produced by the luciferase fusion constructs under the control of the AUG*gag* codon (Fig. 3). For each construct, two independent clones were used, giving identical results. Moreover, in several experiments, we showed that mRNAs of the mutants were transcribed to similar levels (Fig. 2).

The 44 nt deletion (Del44) led to a 2-fold increase in translational efficiency at the downstream AUG *gag* codon. The enhanced translation produced by this deletion mimics the effect caused by mutation of AUG3 (2-fold increase; 18). One possible interpretation of this result is that the intercistronic interval is too short to allow efficient reinitiation at AUG3 (34), thus permitting the ribosomes to initiate downstream at the AUG*gag* more efficiently. More surprising was the result obtained for Del13: shortening of the intercistronic space between uORF1 and 3 by

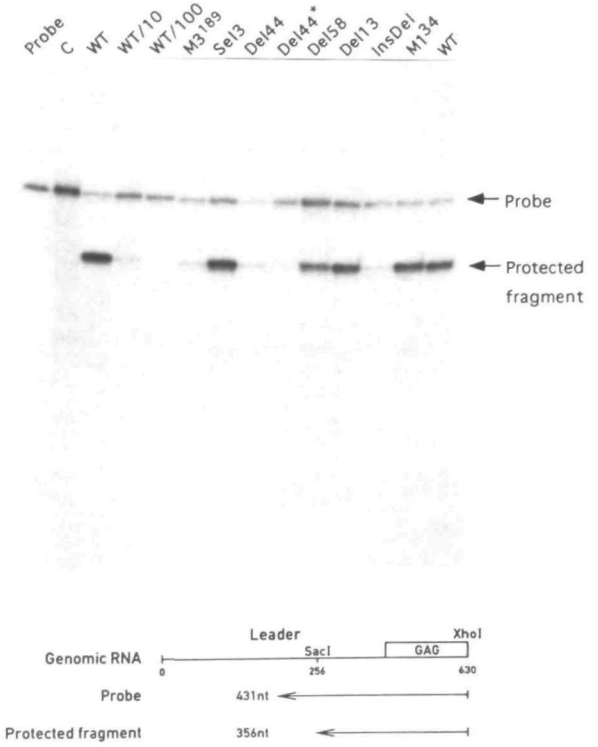

Figure 5. Viral RNA content of the virions produced in a transient transfection assay. At the top is represented a typical RNase protection assay. Protected fragments have been analyzed by electrophoresis in a polyacrylamide sequencing gel. Bands were visualized by autoradiography. The RNA for each virus (wild-type and mutants) was extracted from an equivalent number of virions (normalized to CA protein, Fig. 4). Names of the different virus are indicated above the lanes. Lane WT/10 and WT/100 indicate 1:10 and 1:100 dilutions of RNA extracted from the WT virions, respectively. Lane C indicates control cells. Undigested probes and protected fragments are indicated on the right. A schematic illustration of the probe used in this experiment is shown below. The protected fragments covers the region from nucleotide positions 630–256. The full-length probe contains an additional 75 nt from Bluescript plasmid (Stratagene).

only 13 nt had a similar effect on translational activity at AUG*gag*, as did deletion of 44 nt (a 2-fold increase in the production of luciferase compared to wt).

The presence of a new chimeric uORF1 terminating at ~70 nt upstream of AUG3 (Del58) increased translation at the AUG*gag* by 2-fold relative to wild-type (Fig. 3), as observed for Del44. The mutant $M3^{189}$, with a new uORF3 situated 11 nt upstream of the bona fide AUG3, also showed a 2-fold increase in translation. Accordingly, this novel AUG3, although demonstrating a acceptable sequence context, seems to be bypassed by ribosomes. These data emphasize the importance of the intercistronic interval between uORF1 and 3 since a deletion as short as 13 nt impairs the ability of uORF3 to inhibit scanning ribosomes. The intercistronic minimal distance which can be deleted could be shortened to 9 nt in the case of $M3^{189}$, but because the AUG3 of this mutant is different than the WT AUG3, we cannot compare its intercistronic distance requirement to the other deletion mutants.

If the intercistronic distance were indeed the sole factor influencing reinitiation at AUG3 or translational regulation at AUG*gag*, then restoration of the wt intercistronic length should allow ribosomes to initiate at AUG3, thereby inhibiting translation initiation at AUG*gag*. To test this prediction, we inserted 94 nt into Del44 between uORF1 and uORF3 at a place devoid of assigned function (position 102; see InsDel: Fig. 3). Thus, this leader carries a 94 nt insertion coupled with a 44 nt deletion, to rebuild an intercistronic distance greater than the wt distance. The new hybrid intercistronic interval restored completely the reinitiation competence of the ribosomes to wild-type level (Fig. 3), revealing that a longer distance between uORF1 and uORF3 does not favor more efficient reinitiation. Accordingly, 134 nt appears to be the preferred reinitiation distance for the virus: increasing it does not enhance reinitiation efficiency, whereas deletion of only 13 nt strongly impairs reinitiation. The experiments presented here are consistent with the idea that reinitiation is distance-dependent and strongly suggest that reinitiation is involved in RSV translational regulation.

Deletions between uORFs in the RSV leader decrease RSV RNA encapsidation to different extents

RNA packaging in avian retroviruses requires specific *cis*-sequences located within the 5′ leader (8–10). As the different mutants designed in this study are located near the proposed packaging signal (Fig. 3), we were interested to study the effect of each deletion on the RSV RNA packaging. To this end, the mutations were inserted into the RSV genome (pAPr-C strain) and studied *in vivo* by transfecting the plasmids into chicken embryo fibroblasts (see Materials and Methods and ref. 18). The particles were purified and quantitated by Western immunoblotting (Fig. 4). The RNA was extracted from an equivalent amount of virions (normalized against the CA protein: Fig. 4) for each mutant and analyzed by RNase protection. A typical result obtained with our packaging assays is shown in Figure 5. The mutant Del58, lacking a large portion of the U5 sequence, demonstrates a slight reduction in RNA packaging (40–50% as compared to wild-type). The Sel3 mutant carrying a lengthened version of the uORF3 ressembles the $pAM3^{224}$ mutant (described in ref. 18) and showed no defect in viral RNA packaging. Both mutants have an uORF3 which terminates in, or overlaps with the ψ packaging sequence without affecting RNA encapsidation. The mutant del13 contains normal amount of viral RNA within the virion, while the Del44 and InsDel mutants packaged ~5–10% of viral RNA as compared as WT. This deletion encompasses nucleotides 160–167 which are part of a stem–loop structure that has been recently shown to be crucial for viral RNA packaging (38). Finally, removal of AUG3 plus the creation of a new AUG ($M3^{189}$; Fig. 5) decrease packaging to >5% as already observed for the pAM3 mutant lacking the third AUG (18). These results support the idea that sequences other than those already described are involved during the packaging step of the RSV infectious cycle.

DISCUSSION

In our previous study, we showed that mutations in the AUG codons of the upstream open reading frames of RSV influence translation and have a profound effect on the viral RNA packaging. Elucidation of the mechanism by which these uORFs influenced these processes required a better understanding of events occuring at each of the AUGs on the RSV leader. The present study was aimed at defining more precisely the transla-

tional events at the short open reading frames, using luciferase fusion constructs. In addition, we designed specific deletions in order to investigate the potential importance of reinitiation at AUG3 for translation.

Here, we report that AUG1, which is the main ribosome binding site within the RSV leader (12,13), is also the most efficient translation initiation site (Fig. 1). This AUG, surrounded by a poor initiation context according to Kozak (31) is situated at an ideal consensus distance from the 5′ cap (40 nt) and followed by a stable secondary structure (36,37). These two factors are known to potentiate recognition at an AUG by scanning ribosomes (1). In our fusion construct, we probably disrupted part of the secondary structure which is possibly involved in assisting ribosomes to initiate at AUG1. However, we found a 4-fold increase in initiation at AUG1 under these minimal conditions. It is therefore possible that measuring the heptapeptide in its natural context would show even greater stimulation. For uORF3, our data show a high incidence of initiation at that AUG in the fusion study as well as in the Sel3 mutant (and in ref. 18, pAM3 and pAMUP). The role of AUG2 as an initiation site has been dismissed by our studies, but this conclusion seems to disagree with the data from another lab (29). It is worth noting that different avian strains are used (SR-A and Pr-C), although the sequence around the AUG2 is conserved between both strains. However in their translational study which showed the effect of uORF2 when it was elongated, Hackett and collaborators used a truncated version of the RSV leader which could be the source of the discrepancy between their results and ours (29). Moreover, in an avian mutant (TK15), uORF2 is elongated, overlapping the AUG*gag*. Translation was not affected in this mutant, supporting the observation that AUG2 is not recognized by the ribosomes (39).

So we can depict the following scheme for translation on RSV leader: following translation of the first uORF, ribosomes mostly resume scanning to reinitiate at the third AUG situated 134 nt further downstream (see Fig. 1: BsAUG3luc, BsORF3luc and Fig. 3, Sel3). From the Sel3 mutant we can conclude that for two ribosomes that initiate at AUG3, one passes through the uORF. Therefore both leaky scanning and reinitiation are involved in the translational regulation of RSV gene expression. Our results are consistent with AUG1 as the major translation initiation site on the RSV leader and AUG3 as being recognized with high efficiency. This is similar to the GCN4 leader, however, in the GCN4 system most ribosomes which reinitiate at downstream uORFs dissociate from the mRNA (26). Whereas in RSV, after translation of uORF3, ribosomes can still resume scanning to reinitiate at AUG*gag* (Fig. 1 BsWT).

In Rous sarcoma virus RNA, the distance between uORF1 and uORF3 (134 nt) is well conserved between the different avian/leukosis retrovirus strains (7,35). The conservation of the intercistronic distance is consistent with our reinitiation model. Indeed, as observed with deletion mutants (13 and 44 nt deletions), the intercistronic interval in RSV leader must be kept constant for efficient reinitiation at AUG3 and hence for translational regulation at AUG*gag*. This agrees with other studies on reinitiation, where it was reported that the inhibitory effect of inserting a single uORF on translation of downstream product decreases as the uORF is moved further upstream (27). To explain this observation, it was suggested that ribosomes scanning from the uORF's termination codon to a downstream start codon require a certain period of time to bind a new set of initiation factors (34). In a mammalian system, 79 nt was found to be a sufficient interval, while in yeast, especially under starvation conditions and in plant cells, a longer spacing is preferred (26,40). In RSV, the distance requirement is between that for yeast and preproinsulin and can be modulated depending on the uORF present on the leader (see below).

Taken together with results from previous studies on RSV, our data are consistent with a role for uORFs in determining the degree of reinitiation. Variations in the optimal intercistronic distance can be seen in RSV. For example, the RSV mRNA encoding the *src* gene, contains a 63 nt intercistronic distance which is sufficient for alleviating the inhibitory effect of an uORF (41). Thus, in the same virus and in the same cell (avian fibroblasts), ribosomal subunits require different intercistronic intervals to become competent for reinitiation (134 versus 63 nt). Differences in reinitiation competence have been well documented in the GCN4 gene of the yeast *Saccharomyces cerevisiae* where it has been shown that certain intrinsic properties of an uORF may be important in determining the efficiency of downstream reinitiation and translation. The proximal region close to the termination codon is crucial, in particular, A + U rich sequences in this region favor reinitiation (42–44). Nevertheless, it seems that this sequence determinant cannot be generalized to higher eukaryotic systems, since in RSV, the analogous region surrounding the uORF stop codon is not A + U rich. The exact features of the uORFs that allow for this type of regulation remain to be elucidated.

In a recent report, we mentioned that uORFs 1 and 3 regulate RNA packaging, presumably through their translational properties (18). The data presented here are in agreement with such a role since both uORF1 and 3 but not uORF2 are efficiently translated. With respect to the mechanism by which these uORFs act, one possibility is that ribosome pausing at AUG3 would impede temporarily the flow of ribosomes on the RSV leader, clearing the ψ packaging sequence present in the leader just downstream of uORF3 (18); but this model is weakened by the leaky scanning occuring at AUG3 shown in this study (Fig. 3: Sel3) Another possible mechanism that has been postulated recently involves the ability of the ψ sequence to form a stem–loop structure (7,38) which can be alternatively folded by base-pairing to uORF3 (7). The authors postulated that ribosomes translating uORF3 sequence could negatively regulate packaging by disrupting the secondary structure, but they assumed that AUG3 is poorly translated (29). Our data show directly that uORF3 is efficiently translated (Fig. 1: BsAUG3 and BsORF3luc, and Fig. 3: Sel3). For this reason, we postulate that translation of uORF3 is a prerequisite for packaging by the disruption of an inhibitory secondary structure, thus allowing binding of the Pr76*gag* to the ψ region. This model could explain the conservation of uORFs in the RSV leader rich in secondary structure and that efficient translation initiation of these upstream AUGs supports a function in melting structured RNA (7,18).

ACKNOWLEDGEMENTS

We thank Andrew Craig, Greg Cosentino, Sylvie Mader and Robert Frederickson for critical reading of the manuscript. We are grateful to Nicholas Roggli for drawings and photographs and to Danièle Rifat for synthesis of oligonucleotides. One of us (OD) gratefully acknowledges the financial support of the Sandoz Stiftung, Basel, Switzerland. This work was supported by grant 31.29983.90 from the Swiss National Science foundation.

REFERENCES

1 Kozak, M. (1989) *J. Cell. Biol.*, **108**, 229–241.
2 Merrick, W.C. (1992) *Microbiol. Rev.*, **56**, 291–315.
3 Damiani, R.D. and Wessler, S.R. (1993) *Proc. Natl. Acad. Sci. USA*, **90**, 8244–8248.
4 Degnin, C.R., Schleiss, M.R., Cao J. and Geballe, A.P. (1993) *J. Virol.*, **67**, 5514–5521.
5 Hill, J.R and Morris, D.R. (1993) *J. Biol. Chem.*, **268**, 726–731.
6 Werner, M., Feller, A., Messenguy, F. and Pierard, A. (1987) *Cell*, **49**, 805–813.
7 Hackett, P.B., Dalton, M.W., Johnson, D.P. and Petersen, R. (1992) *Nucleic Acids Res.*, **19**, 6929–6934.
8 Linial, M. and Miller,A.D. (1990) *Curr. Topics Microbiol. Immunol.*, **157**, 125–152.
9 Katz, R.A., Terry, R.W. and Skalka, A.M. (1986) *J. Virol.*, **59**, 163–167.
10 Aronoff, R., Hajjar, A.M. and Linial, M.L. (1993) *J. Virol.*, **67**, 178–188.
11 Darlix, J.L., Spahr, P.F., Bromley, P.A. and Jaton, J.C. (1979) *J. Virol.*, **29**, 597–611.
12 Petersen, R. B., Hensel, C.M. and Hackett, P.B. (1984) *J. Virol.*, **51**, 727–729.
13 Petersen, R. B. and Hackett, P.B. (1985) *J. Virol.*, **56**, 683–690.
14 Hackett, P. B., Petersen, R. B. , Hensel, C. H. , Albericio, F., Gunderson, S. I., Palmenberg, A. C. and Barany, G. (1986) *J. Mol. Biol.*, **190**, 45–57.
15 Hensel, C. H., Petersen, R. B. and Hackett, P.B. (1989) *J. Virol.*, **63**, 4986–4990.
16 Moustakas, A., Sonstegard, T.S. and Hackett, P.B. (1993) *J. Virol.*, **67**, 4337–4349.
17 Petersen, R. B., Moustakas, A. and Hackett, P.B. (1989) *J. Virol.*, **63**, 4787–4796.
18 Donzé, O. and Spahr, P.F. (1992) *EMBO J.*, **11**, 3747–3757.
19 Sambrook, J., Fristch E. F. and Maniatis, T. (1989) *Molecular Cloning: A Laboratory Manual* (2nd ed.). Cold Spring Harbor University Press, Cold Spring Harbor, NY.
20 Méric, C. and Spahr,P.F. (1986) *J. Virol.*, **60**, 450–459.
21 De Wet, J.R., Wood, K.W., DeLuca, M., Helinski, D.R. and Subramani, S. (1987) *Mol. Cell. Biol.*, **7**, 725–737.
22 Oertle, S. and Spahr, P.F. (1990) *J. Virol.*, **64**, 5757–5763.
23 Lo, K. M., Jones, S.S., Hackett, N. and Khorana, H.G. (1984) *Proc. Natl. Acad. Sci. USA.*, **81**, 2285–2289.
24 Kunkel, T. A. (1985) *Proc. Natl. Acad. Sci. USA.* **82**, 488–492.
25 Hinnebusch, A.G. (1988) *Proc. Natl. Acad. Sci. USA*, **85**, 7279–7283.
26 Abastado, J.P., Miller, P.F., Jackson, B.M. and Hinnebusch A.G. (1991) *Mol. Cell. Biol.*, **11**, 486–496.
27 Fütterer, J. and Hohn, T. (1992) *Nucleic Acids Res.*, **20**, 3851–3857.
28 Peabody, D.S. and Berg, P. (1986) *Mol. Cell. Biol.*, **6**, 2695–2703.
29 Moustakas, A., Sonstegard, T.S. and Hackett, P.B. (1993) *J. Virol.*, **67**, 4350–4357.
30 Kozak. M. (1986) *Proc. Natl. Acad. Sci. USA*, **83**, 2850–2854.
31 Kozak, M. (1991) *J. Cell. Biol.*, **115**, 887–903.
32 Pelletier, J. and Sonenberg, N. (1985) *Cell*, **40**, 515–526.
33 Pelletier, J. and Sonenberg, N. (1988) *Nature*, **334**, 320–325.
34 Kozak, M. (1987) *Mol. Cell. Biol.*, **7**, 3438–3445.
35 Bizub, D., Katz, R. A. and Skalka, A.M. (1984) *J. Virol*, **49**, 557–565.
36 Cobrinik, D., Sosky, L. and Leis, J. (1988) *J. Virol.*, **62**, 3622–3630.
37 Cobrinik, D., Aiyar, A., Ge, Z., Katzman, M., Huang, H. and Leis, J. (1991) *J. Virol.*, **65**, 3864–3872.
38 Knight, J.B., Si, Z.H and Stoltzfus, C.M. (1994) *J. Virol.*, **68**, 4493–4502.
39 Kawai, S and T. Koyama. (1984) *J. Virol.*, **51**, 147–153.
40 Fütterer, J. and Hohn, T. (1991) *EMBO J.*, **10**, 3887–3896.
41 Hughes, S., Mellstrom, K., Kosik, E., Tamanoi, F. and Brugge, J. (1984) *Mol. Cell Biol.*, **4**, 1738–1746.
42 Grant, C.M. and Hinnebusch, A.G. (1994) *Mol. Cell. Biol.*, **14**, 606–618.
43 Miller, P. F. and Hinnebusch, A.G. (1989) *Genes Dev.*, **3**, 1217–1225.
44 Mueller, P.F., Jackson, B.M., Miller, P.F. and Hinnebusch, A.G. (1988) *Mol. Cell. Biol.*, **8**, 5439–5447.